Ruthenium(0) Nanoclusters Stabilized by a Nanozeolite Framework: Isolable, Reusable, and Green Catalyst for the Hydrogenation of Neat Aromatics under Mild Conditions with the Unprecedented Catalytic Activity and Lifetime

Mehmet Zahmakıran, Yalçın Tonbul,[†] and Saim Özkar*

Department of Chemistry, Middle East Technical University, Ankara 06531, Turkey

Received February 24, 2010; E-mail: sozkar@metu.edu.tr

Abstract: The hydrogenation of aromatics is a ubiquitous chemical transformation used in both the petrochemical and specialty industry and is important for the generation of clean diesel fuels. Reported herein is the discovery of a superior heterogeneous catalyst, superior in terms of catalytic activity, selectivity, and lifetime in the hydrogenation of aromatics in the solvent-free system under mild conditions (at 25 °C and 42 ± 1 psig initial H_2 pressure). Ruthenium(0) nanoclusters stabilized by a nanozeolite framework as a new catalytic material is reproducibly prepared from the borohydride reduction of a colloidal solution of ruthenium(III)-exchanged nanozeolites at room temperature and characterized by using ICP-OES, XRD, XPS, DLS, TEM, HRTEM, TEM/EDX, mid-IR, far-IR, and Raman spectroscopy. The resultant ruthenium(0) nanoclusters hydrogenate neat benzene to cyclohexane with 100% conversion under mild conditions (at 25 °C and 42 ± 1 psig initial H_2 pressure) with record catalytic activity (*initial* TOF = 5430 h^{-1}) and lifetime (TTO = 177 200). They provide exceptional catalytic activity not only in the hydrogenation of neat benzene but also in the solvent-free hydrogenation of methyl substituted aromatics such as toluene, *o*-xylene, and mesitylene under otherwise identical conditions. Moreover, they are an isolable, bottleable, and reusable catalyst in the hydrogenation of neat aromatics. When the isolated ruthenium(0) nanoclusters are reused, they retain 92% of their initial catalytic activity even for the third run in the hydrogenation of neat benzene under the same conditions as those of the first run. The work reported here also includes (*i*) far-infrared spectroscopic investigation of nanozeolite, ruthenium(III)-exchanged-nanozeolite, and ruthenium(0) nanoclusters stabilized by a nanozeolite framework, indicating that the host framework remains intact after the formation of a nanozeolite framework stabilized ruthenium(0) nanoclusters; (*ii*) the poisoning experiments performed by using tricyclohexylphosphine (P(C$_6$H$_{11}$)$_3$) and 4-ethyl-2,6,7-trioxa-1-phosphabicyclo[2.2.2]octane PC$_6$H$_{11}$O$_3$ to examine whether the ruthenium(0) nanoclusters are encapsulated in the cages or supported on the external surface of nanozeolite; (*iii*) a summary section detailing the main findings for the "green chemistry"; and (*iv*) a review of the extensive literature of benzene hydrogenation, which is also tabulated as part of the Supporting Information.

Introduction

The complete hydrogenation of aromatics is one of the most important and challenging transformations in the synthesis of fine chemicals and intermediates[1] and, traditionally, has been carried out at high temperature (>100 °C) and/or high pressure (50 atm H$_2$).[2] Literature review reveals that a range of homogeneous and heterogeneous catalysts have been used to hydrogenate benzene. Among these, the catalysts[3] that achieve the complete hydrogenation of benzene without any side products under mild conditions ($\leq$25 °C and $\leq$3 atm H$_2$) are the hydroxyalkylammonium halide stabilized rhodium(0)[4] and iridium(0) nanoclusters,[5] cyclodextrins stabilized rhodium(0)

nanoclusters,[6] rhodium(0) nanoclusters immobilized on silica,[7] Rh(COD) moiety anchored to polymers,[8] rhodium(0) nanoclusters entrapped in boehmite nanofibers,[9] ruthenium(0) nanoclusters immobilized into SBA-15,[10] [(Cp*)$_2$Zr(CH$_3$)$_2$]$^+$ activated

---

† On leave of absence from Dicle University, 21280, Diyarbakır, Turkey

(1) (a) Larock, R. C. *Comprehensive Organic Transformations*; Wiley-VCH: New-York, 1999. (b) Sheldon, R. A.; Kochi, J. K. *Metal Catalyzed Oxidation of Organic Compounds*; Academic: New York, 1981.

(2) Augustine, R. L. *Heterogeneous Catalysis for the Synthetic Chemistry*; Marcel Dekker: New York, 1996.

(3) A SciFinder literature search confirms that ca. 95% of the reports of benzene hydrogenation catalysis employ high temperature and/or high pressure with only 5% (90 of >1900) hits refining according to the terms "benzene hydrogenation at room temperature". Of the 95 hits, 17 report the complete (100%) hydrogenation of benzene without side products at room temperature, and they were tabulated in Table S-1 in the Supporting Information.

(4) (a) Schulz, J.; Patin, H.; Roucoux, A. *Chem. Commun.* **1999**, 535. (b) Schulz, J.; Patin, H.; Roucoux, A. *Chem.—Eur. J.* **2000**, *6*, 618. (c) Schulz, J.; Patin, H.; Roucoux, A. *Adv. Synth. Catal.* **2003**, *345*, 222.

(5) Mevellec, V.; Ramirez, E.; Philippot, K.; Chaudret, B.; Roucoux, A. *Adv. Synth. Catal.* **2004**, *346*, 72.

(6) Nowicki, A.; Zhong, Y.; Leger, B.; Rolland, J. P.; Bricout, H.; Monflier, E.; Roucoux, A. *Chem. Commun.* **2006**, 296.

(7) Roucoux, A.; Philippot, K.; Payen, E.; Granger, P.; Dujardin, C.; Nowicki, A.; Mevellec, V. *New J. Chem.* **2006**, *30*, 1214.

(8) Seeberger, M. H.; Jones, R. A. *J. Chem. Soc., Chem. Commun.* **1985**, *6*, 373.

via super acidic sulfated alumina or sulfated zirconia,[11] intrazeolite ruthenium(0) nanoclusters,[12] rhodium(0) nanoclusters stabilized by polyhydroxylated ammonium chloride,[13] and CNT-supported rhodium(0) nanoclusters[14] (see Table S-1 in the Supporting Information). As a common feature, all of these catalytic systems, except Mark's catalyst,[11] involve transition metal nanoclusters catalysts, which have attracted much attention in organic synthesis due to their distinct catalytic activities for various transformations.[15] However, in their catalytic application one of the most important problems is the aggregation of nanoclusters into clumps and ultimately to the bulk metal, despite using the best stabilizers,[16] which leads to a momentous decrease in catalytic activity and lifetime. The use of nanocluster catalysts in systems with confined void spaces such as inside mesoporous and microporous solids appears to be an efficient way of preventing aggregation.[12,17] Expectedly, our previous study[12] has shown that zeolite confined ruthenium(0) nanoclusters provide record catalytic activity in the hydrogenation of neat benzene under mild conditions (22 °C, 42 ± 1 psig H_2). Further improvement in the catalytic activity is rationally expected by reducing the particle size of zeolite-Y, as the diffusion of the substrate molecules through the cavities from the external surface to the cages, where the nanoclusters reside, can limit the reaction rate. A decrease in the particle size of host material results in high external surface areas and, thus, reduces the diffusion path length compared to the large size zeolite crystals (≥ 1 μm). With this anticipation, we employed the nanoparticles of zeolite-Y with a narrow size distribution[18,19] as the host for the stabilization of metal(0) nanoclusters.

Herein, we report the preparation and characterization of ruthenium(0) nanoclusters stabilized by a nanozeolite framework as a novel catalytic material. They were reproducibly prepared from the borohydride reduction of a colloidal solution of ruthenium(III)-exchanged nanozeolites at room temperature. The composition, morphology, and structure of the nanozeolite framework stabilized ruthenium(0) nanoclusters, as well as the integrity and crystallinity of the host material, were investigated by using ICP-OES, XRD, XPS, DLS, TEM, HRTEM, TEM/EDX, mid-IR, far-IR, and Raman spectroscopy. The results of these multiprong analyses combined with poisoning experiments with phosphine ligands (*vide infra*) reveal the formation of ruthenium(0) nanoclusters within the zeolite cages as well as on the external surface of a nanozeolite without causing an alteration in the framework lattice or loss in the crystallinity of the host material. Ruthenium(0) nanoclusters stabilized by a nanozeolite framework were found to be the most active (*initial* turnover frequency (TOF) = 5430 h^{-1}) and longest lifetime (*total* turnovers, TTO = 177 200) catalyst ever reported for the complete hydrogenation of neat benzene under mild conditions (at 25 °C and 42 ± 1 psig initial H_2 pressure). They also provide exceptional catalytic activity in the complete hydrogenation of methyl substituted arenes such as toluene, *o*-xylene, and mesitylene in the solvent-free systems under otherwise identical conditions. Moreover, the ruthenium(0) nanoclusters exhibit high durability throughout their catalytic use in the hydrogenation reaction against agglomeration and leaching. This significant property makes them a reusable catalyst in the hydrogenation of aromatics without appreciable loss of their inherent activity. More importantly, they fulfill the majority of the "Green Chemistry" requirements[20] which impose neat/solventless systems whenever possible. There are only seven reports for the complete conversion of neat benzene to cyclohexane at temperatures $\leq$25 °C.[8–14] The work reported here also includes poisoning experiments performed using the large tricyclohexylphosphine ($P(C_6H_{11})_3$) or the compact 4-ethyl-2,6,7-trioxa-1-phosphabicyclo[2.2.2]octane ($PC_6H_{11}O_3$) to determine the distribution of ruthenium(0) nanoclusters between the cavities and the external surface of a nanozeolite.

Experimental Section

Materials. Ruthenium(III) chloride trihydrate ($RuCl_3 \cdot 3H_2O$), sodium borohydride ($NaBH_4$, 98%), tetramethylammonium hydroxide solution (($CH_3)_4NOH$, 25% wt), aluminum propan-2-olate ($Al(OC_3H_7)_3$, >98%), tetramethylammonium bromide (($CH_3)_4NBr$, >98%), aqueous 30% wt colloidal silica (LUDOX HS-30, $SiO_2/Na_2O = 90$, % wt $SiO_2 = 29.90$, % wt $Na_2O = 0.34$), benzene (99%), toluene (99%), and d-Chloroform ($CDCl_3$) were purchased from Aldrich. Mesitylene (98%) and *o*-xylene (98%) were purchased from Fluka. All catalyst reaction solutions were prepared in an oxygen-free atmosphere (Labconco, drybox). Benzene, toluene, mesitylene, and *o*-xylene were distilled over sodium under argon and stored in the drybox. Ruthenium(III) chloride was recrystallized from water, and the water content of $RuCl_3 \cdot xH_2O$ was determined by TGA and found to be $x = 3$. Deionized water was distilled by a water purification system (Milli-Q System). All glassware and Teflon coated magnetic stir bars were cleaned with acetone, followed by copious rinsing with distilled water before drying in an oven at 150 °C. Polypropylene bottles were washed with doubly deionized water under ultrasonication.

Preparation of Ruthenium(0) Nanoclusters Stabilized by a Nanozeolite Framework. The colloidal nanozeolites (FAU-type) were prepared from a clear precursor solution with the molar composition 1.00 Al_2O_3:4.36 SiO_2:2.39 $(TMA)_2O(2$ OH^-):1.2 $(TMA)_2O(2$ Br^-):0.048 Na_2O:249 H_2O (weight composition is as follows: 38.3 g of H_2O, 26.2 g of TMAOH, 5.7 g of TMABr, 6.3 g of Al(*i*-OPr)$_3$, and 13.1 g of Ludox HS-30) as described elsewhere.[21] After complete crystallization of the solution, the resulting colloidal nanozeolite crystals were recovered by three repetitions of high speed centrifugation (12 000 rpm for 1 h), decantation, and redispersion in doubly distilled water at room temperature. Then, to remove sodium defect sites, colloidal nanozeolites were ion-exchanged[22] with 100 mL of 1 M NaCl solution at 50 °C for 12 h and recovered again by three cycles of high speed centrifugation (12 000 rpm for 1 h), decantation, and redispersion in doubly

(9) Park, I. S.; Kwon, M. S.; Kim, N.; Lee, J. S.; Kang, K. Y.; Park, J. *Chem. Commun.* **2005**, 5667.

(10) Zhang, J.; Xie, Z.; Liu, Z.; Wu, W.; Han, B.; Huang, J.; Jiang, T. *Catal. Lett.* **2005**, *103*, 59.

(11) Nicholas, J. P.; Ahn, H.; Marks, T. J. *J. Am. Chem. Soc.* **2003**, *125*, 4325.

(12) Zahmakıran, M.; Özkar, S. *Langmuir* **2008**, *24*, 7065.

(13) Hubert, C.; Denicourt-Nowicki, A.; Guégan, J.-P.; Roucoux, A. *Dalton Trans.* **2009**, 7356.

(14) Pan, H. B.; Wai, C. M. *J. Phys. Chem. C* **2009**, *113*, 19782.

(15) (a) Schmid, G. In *Nanoparticles: From Theory to Application*; Wiley-VCH: Weinheim, 2004. (b) Widegren, J. A.; Finke, R. G. *J. Mol. Catal. A: Chem.* **2003**, *191*, 187. (c) Widegren, J. A.; Finke, R. G. *J. Mol. Catal. A: Chem.* **2003**, *198*, 317.

(16) Özkar, S.; Finke, R. G. *J. Am. Chem. Soc.* **2002**, *124*, 5796. (b) Özkar, S.; Finke, R. G. *Langmuir* **2002**, *18*, 7653.

(17) (a) Seidel, A.; Loos, J.; Boddenberg, B. *J. Mater. Chem.* **1999**, *9*, 2495. (b) Tang, Q.; Zhang, Q.; Wang, P.; Wang, Y.; Wan, H. *Chem. Mater.* **2004**, *16*, 1967. (c) Zahmakıran, M.; Özkar, S. *Langmuir* **2009**, *25*, 2667. (d) Zahmakıran, M.; Özkar, S. *Appl. Catal., B* **2009**, *84*, 104. (e) Çalışkan, S.; Zahmakıran, M.; Özkar, S. *Appl. Catal., B* **2010**, *93*, 387.

(18) The nanosized zeolites are usually defined as the highly crystalline zeolites that have a size of less than 1000 nm (see ref17).

(19) Tosheva, L.; Valtchev, V. P. *Chem. Mater.* **2005**, *17*, 2494.

(20) Poliakoff, M.; Fitzpatrick, J. M.; Farren, T. R.; Anastas, P. T. *Science* **2002**, *297*, 807.

(21) Holmberg, B. A.; Wang, H.; Norbeck, J. M.; Yan, Y. *Microporous Mesoporous Mater.* **2003**, *59*, 13.

(22) Breck, D. W. *Zeolite Molecular Sieves*; Krieger: Malabal, FL, 1984.

distilled water at room temperature. Next, they were ion-exchanged with Ru^{3+} cations in 100 mL of aqueous solution of $RuCl_3$ (26.1 mg, 0.1 mmol) for 12 h at 50 °C. The solution was then cooled down to room temperature, and ruthenium(III) cations were reduced by the addition of 10 mmol of $NaBH_4$ (378 mg). The reduction was considered to be complete when no more hydrogen evolution was observed (~10 min). Then, this mixture was centrifuged at 5000 rpm for 30 min, and the solid was separated from the solution by decantation and washing with 200 mL of doubly distilled water. The final product was dried under vacuum (10^{-3} Torr) at 90 °C for 6 h and stored in a glovebox.

Characterization of Nanozeolite Framework Stabilized Ruthenium(0) Nanoclusters. The chemical composition of the samples was determined by inductively coupled plasma atomic emission spectroscopy (ICP-AES; Varian-Vista) after each sample was completely dissolved in the mixture of HNO_3/HCl with a 1:3 ratio. Powder X-ray diffraction (XRD) patterns were acquired on a MAC Science MXP 3TZ diffractometer using Cu Kα radiation (wavelength 1.5406 Å, 40 kV, 55 mA). Dynamic light scattering (DLS) measurements in colloidal suspensions were performed with a Malvern Zetasizer-Nano instrument equipped with a 4 mW He−Ne laser (633 nm) and an avalanche photodiode detector. Transmission electron microscopy (TEM) and high resolution TEM (HRTEM) analyses were performed on a JEM-2010F microscope (JEOL) operating at 200 kV. The TEM/EDX elemental analysis was performed by using an energy dispersive X-ray (EDX) analyzer (KEVEX Delta series) mounted on the Hitachi S-800 modulated to TEM. XPS analysis was performed on a Physical Electronics 5800 spectrometer equipped with a hemispherical analyzer and using monochromatic Al Kα radiation (1486.6 eV, the X-ray tube working at 15 kV, 350 W and pass energy of 23.5 keV). NMR spectra were recorded on a Bruker Avance DPX 400 (400.1 MHz for ^1H). FTIR spectra were recorded under N_2 gas purging using a Nicolet Magna-IR 750 spectrometer. The Raman spectrum of the sample was recorded on a Bruker RFS-100/S series Raman spectrometer equipped with a Nd:YAG laser at 1064 nm using the FT-Raman technique.

Pretreatment of the Samples and Measurement Conditions for the Far-IR Experiments. For the far-IR analyses, samples of nanozeolite, ruthenium(III)-exchanged nanozeolite, and its reduced form, nanozeolite framework stabilized ruthenium(0) nanoclusters, were prepared by following the procedure described in the section "Preparation of Ruthenium(0) Nanoclusters Stabilized by Nanozeolite Framework". The samples were pressed into self-supporting wafers of 15 mm in diameter weighing approximately 15 mg by using an applied pressure of 6−8 tons per square inch for up to 60 s. The wafers were clamped into a glass tube whose one side was connected to a turbo-molecular vacuum pump and placed in a furnace. The self-supporting wafers were dehydrated with the following schedule, using an NX-(Mitsubishi) series temperature controller: 0.5 h from 25 to 100 °C, 1 h at 100 °C, 4 h from 100 to 550 °C, and 4 h at 550 °C. After thermal treatment the samples inside the glass tube were cooled down to room temperature, then sealed, and transferred into the glovebox ($0_2 <$ 5 ppm, $H_2O <$ 1 ppm), where the sample was transferred into a sample holder equipped with a high density polyethylene window. The level of dehydration was checked by complementary mid-IR spectroscopy. The degree of dehydration was judged by the flatness of the baseline in the IR $\nu(OH)$ stretching and $\delta(OH)$ deformation regions, 3400−3700 and 1600−1650 cm^{-1}, respectively.[22] The far-IR spectra were recorded on a Nicolet Magna-IR 750 spectrometer under N_2 purging by using a global source and DTGS detector. The spectral resolution in all cases was 4 cm^{-1}, and all of the spectra have been baseline corrected.

General Procedure for the Hydrogenation of Aromatics Catalyzed by Ruthenium(0) Nanoclusters Stabilized by a Nanozeolite Framework. All reaction mixtures were prepared in a nitrogen-filled oxygen-free drybox ($0_2 <$ 5 ppm, $H_2O <$ 1 ppm) following the procedure described elsewhere.[12] In a drybox the

catalyst was weighed into a 40 mm × 20 mm borosilicate culture tube containing a 5/16 in. × 5/8 in. Teflon coated magnetic stir bar, and then the substrate was added with a gastight syringe. The culture tube was then placed inside the Fischer−Porter (FP) pressure bottle. The FP bottle was sealed, brought outside the drybox, placed inside a constant temperature circulating water bath at 25 ± 0.1 °C, and connected via Swagelock TFE-sealed quick-connects to the hydrogenation line which had already been evacuated for at least 30 min to remove any trace oxygen and water present and then refilled with purified H_2 at 42 ± 1 psig. Then, the FP bottle was purged 10 times (15 s per purge, with stirring at >600 rpm). The pressure in the FP bottle was then set to a constant 42 ± 1 psig H_2, and the reaction was started. The reaction was followed by monitoring the pressure change in the FP bottle via an RS-232 module and using a Lab View 8.0 program on a PC. The pressure vs time data were processed using Microsoft Office Excel 2003 and Origin 7.0. Reaction rates were determined from the slope of the linear portion of the H_2 uptake curve. The complete hydrogenation of each substrate was also confirmed by a ^1H NMR spectrum of the reaction solution taken at the end of the reaction.

Testing the Catalytic Activity of Ruthenium Free Nanozeolite in the Hydrogenation of Neat Benzene. In a control experiment the catalytic activity of ruthenium free nanozeolite (100 mg) was checked in the hydrogenation of 1.0 mL of benzene (under 42 ± 1 psig initial H_2 pressure at 25 ± 0.1 °C), which was performed in the same way as described in the section "General Procedure for the Hydrogenation of Aromatics Catalyzed by Ruthenium(0) Nanoclusters Stabilized by a Nanozeolite Framework"

Isolability, Bottleability, and Reusability of Ruthenium(0) Nanoclusters Stabilized by a Nanozeolite Framework in the Hydrogenation of Neat Benzene. After the first run of the hydrogenation of 1.0 mL of benzene (11.2 mmol), catalyzed by 100 mg of ruthenium(0) nanoclusters stabilized by a nanozeolite framework (with a ruthenium loading of 0.27% wt corresponding to 2.7 μmol of Ru), the FP bottle was detached from the line, taken into the drybox, and opened and the suspension in the culture tube was transferred into a Schlenk tube, resealed, and connected to a vacuum line. After the evaporation of volatiles, the solid residue was weighed (90 and 78 mg for the second and third run, respectively) and used again in the hydrogenation of 1.0 mL of benzene (11.2 mmol) under the same conditions (25 ± 0.1 °C and 42 ± 1 psig H_2 initial pressure). The results were expressed as a percentage of catalytic activity of ruthenium(0) nanoclusters retained in the successive runs of neat benzene hydrogenation.

Determination of the Catalytic Lifetime of Ruthenium(0) Nanoclusters Stabilized by a Nanozeolite Framework in the Hydrogenation of Neat Benzene. The catalytic lifetime of ruthenium(0) nanoclusters stabilized by a nanozeolite framework was determined by measuring their total turnover number (TTO) in the hydrogenation of neat benzene. This experiment was started with a 50 mg amount of ruthenium(0) nanoclusters stabilized by a nanozeolite framework (with a ruthenium loading of 0.27% wt corresponding to 1.35 μmol of Ru) and 3 mL of benzene and performed in the same way as described in the section "General Procedure for the Hydrogenation of Aromatics Catalyzed by Ruthenium(0) Nanoclusters Stabilized by a Nanozeolite Framework". When the complete hydrogenation of benzene had been achieved the FP bottle was removed from the line, taken into the drybox, and opened and more benzene (4 mL) was added into the reaction solution; the reaction was continued in this way until no hydrogen uptake was observed.

$P(C_6H_{11})_3$ and $PC_6H_{11}O_3$ Poisoning of Ruthenium(0) Nanocluster Catalysts in the Hydrogenation of Neat Benzene. For the catalyst poisoning experiments two separate stock solutions were prepared by dissolving 18.7 mL of $P(C_6H_{11})_3$ or 3.0 mg of $PC_6H_{11}O_3$ in 10 mL of benzene. Then, 100 mg of catalyst (0.27% wt Ru loaded) were transferred into a 22 mm × 175 mm culture tube containing a $^5/_{16}$ in × $^5/_8$ in. Teflon coated magnetic stir bar. To

this was added an aliquot (40−80 μL) of P(C₆H₁₁)₃ or (216−720 μL) of PC₆H₁₁O₃ stock solution by using a gastight syringe of 100 or 500 μL, respectively, and the total volume of solution was leveled to 1.0 mL by the addition of benzene. The culture tube was then placed in the FP bottle. The FP bottle was then sealed, taken outside the drybox, placed in a constant temperature circulation water bath thermostatted at 25 ± 0.1 °C, and attached to the hydrogenation apparatus via the quick connects, and the solution was stirred for 30 min. Next, the hydrogenation of benzene was carried out in the same way as described in the section of "General Procedure for the Hydrogenation of Aromatics Catalyzed by Ruthenium(0) Nanoclusters Stabilized by a Nanozeolite Framework". In each set the initial rates were calculated in psig/h from the pressure vs time data[23] and used to obtain the percent catalytic activity retained (initial rate of benzene hydrogenation in the presence of poison over the one in the absence of poison multiplied by 100).

Leaching Test of Ruthenium(0) Nanoclusters Stabilized by a Nanozeolite Framework. After the first run of the hydrogenation of 1.0 mL of benzene, catalyzed by 150 mg of ruthenium(0) nanoclusters stabilized by a nanozeolite framework (with a loading of of 0.27% wt Ru, corresponding to 2.7 μmol Ru), the FP bottle was detached from the line, taken into the drybox, and opened and the suspension in the culture tube was filtered; the filtrate was transferred into a new culture tube, and 0.5 mL benzene was added. The culture tube was placed into the FP bottle. The hydrogenation of benzene was performed in the same way as described in the section "General Procedure for the Hydrogenation of Aromatics Catalyzed by Ruthenium(0) Nanoclusters Stabilized by a Nanozeolite Framework". No hydrogenation of benzene was observed after 8 h. Additionally, no ruthenium metal was detected in the filtrate by ICP which had a detection limit of 24 ppb for Ru.

Results and Discussion

Preparation and Characterization of Ruthenium(0) Nanoclusters Stabilized by a Colloidal Nanozeolite Framework. Nanozeolite framework stabilized ruthenium(0) nanoclusters, hereafter referred to as NFS-Ru(0), are prepared as a novel material by a procedure comprising (*i*) the ion exchange[22] of Ru^{3+} ions with the extra framework Na^+ or TMA^+ ions of nanozeolite at 50 °C for 12 h and then (*ii*) the reduction of Ru^{3+} ions in the cavities of a nanozeolite with sodium borohydride in aqueous solution at room temperature, whereby the Na^+ ions reoccupy the cation sites left by the Ru^{3+} ions upon reduction, as tracked by far-IR spectroscopy (*vide infra*). After centrifugation, filtering, copious washing with water, and drying in vacuum at room temperature, NFS-Ru(0) were obtained as gray powders and characterized by ICP-OES and XRD. Comparison of the XRD patterns of nanozeolite and NFS-Ru(0) (see Figure S-1 in the Supporting Information) clearly shows that the host material remains intact with its FAU framework[22] during the preparation. The Bragg reflections of NFS-Ru(0) (with a ruthenium content of 0.27% wt, determined by ICP-OES analysis) are identical with those of the nanozeolite framework.

The high crystallinity, colloidal stability, the degree of polydispersity, and typical morphological appearance of colloidal nanozeolites were investigated by TEM, HRTEM, and DLS analyses. Inspection of the TEM images of the colloidal NFS-Ru(0) samples with a metal loading of 0.27% wt Ru given in Figure 1a and b reveals the following: (*i*) there exist only crystals of colloidal nanozeolite-Y with a crystalline domain size of ∼25 nm which is smaller than that found by DLS measurement[24] (see Figure S-2 in the Supporting Information);

(*ii*) there is no bulk metal formed at an observable size outside the nanozeolite crystals; (*iii*) NFS-Ru(0) are highly dispersible in aqueous medium and colloidal nanozeolites do not aggregate at the end of the preparation of nanoclusters, unlike the results of Mintovas' work,[25] in which the agglomeration of colloidal nanozeolites has been observed in the synthesis of nanozeolite confined copper(0) nanoclusters by a γ-radiolysis method; (*iv*) the method used for the preparation of NFS-Ru(0) does not cause any observable defects in the structure of colloidal nanozeolite-Y, a fact which is also confirmed by XRD results. The HR-TEM image of NFS-Ru(0) given in Figure 1c shows the uniform distribution of ruthenium within the highly ordered cavities of a nanozeolite. A TEM-EDX spectrum of the same sample given in Figure 1d shows that ruthenium is the only element detected[26] in addition to the zeolite framework elements and Cu from the grid. Although no bulk ruthenium metal is observed outside the zeolite nanocrystals, the TEM-EDX and ICP-OES analyses indicate the presence of ruthenium in the samples. This implies that the ruthenium metal is mostly located within the cavities of a colloidal nanozeolite.

The oxidation state of ruthenium and surface composition of the NFS-Ru(0) were analyzed by X-ray photoelectron spectroscopy. The survey scan XPS spectrum of the NFS-Ru(0) sample (see Figure S-3a in the Supporting Information) shows the presence of ruthenium in addition to the zeolite framework elements (O, Si, Al, Na, N, C). The deconvolution of high resolution Ru 3d and 3p XPS spectra of the NFS-Ru(0) sample (see Figure S-3b and c in the Supporting Information) gives three prominent peaks at 285.3, 280.2, and 461.5 eV, readily assigned to Ru(0) $3d_{3/2}$, Ru(0) $3d_{5/2}$, and Ru(0) $3p_{3/2}$, respectively.[27] The peaks observed at 287.6, 281.2, and 463.5 eV show the presence of RuO_2, which may originate from the surface oxidation of ruthenium(0) nanoclusters during the XPS sampling procedure.[28,29] The slight shifts (0.2−0.5 eV) observed in the binding energies of NFS-Ru(0) with respect to ruthenium metal might be attributed to both the quantum size effect[30] and peculiar

(24) DLS analysis gives a unimodal particle size distribution for the NFS-Ru(0) sample, a peak centered at 130 nm as shown in Figure S-2, when the scattering intensity is expressed as number-weighted dependence. It is noteworthy that the particle size measured by considering only the nontouching particle in the TEM image of the same sample is much smaller than that obtained by DLS which accounts for the touching spots as one particle.

(25) Kecht, J.; Tahri, Z.; Waele, V. D.; Mostafavi, M.; Mintova, S.; Bein, T. *Chem. Mater.* **2006**, *18*, 3373.

(26) As judged by the Lα₁, Lα₂ Kα₁, and Kα₂ lines of Ru at 2.61, 2.56, 19.3, and 19.1 keV, respectively: Jones, I. P. *Chemical Microanalysis Using Electron Beams*; The Institute of Materials: London, 1992.

(27) (a) Wagner, C.; Riggs, W. M.; Davis, L. E.; Moulder, J. F.; Muilenberg, G. E. *Handbook of X-ray Photoelectron Spectroscopy*; Physical Electronic Division, Perkin-Elmer: Eden Prairie, MN, 1979; Vol. 55, p 344. (b) Park, K. W.; Choi, J. H.; Kwon, B. K.; Lee, S. A.; Sung, Y. E.; Ha, H. Y.; Hong, S. A.; Kim, H.; Lee, S. A.; Sung, Y. A.; Ha, H. Y.; Hong, S. A.; Kim, H.; Wieckowski, A. *J. Phys. Chem. B* **2002**, *106*, 1869. (c) Nyholm, R.; Maartensson, N. *Solid State Phys.* **1980**, *13*, L279. (d) Chakroune, N.; Viau, G.; Ammar, S.; Poul, L.; Veautier, D.; Chehimi, M. M.; Mangeney, C.; Villain, C.; Fievet, F. *Langmuir* **2005**, *21*, 6788.

(28) Although oxidation of ruthenium(0) nanoclusters during the XPS sampling procedure is a well known fact, the results obtained from XPS analysis need to be tested by using other analytical techniques to check whether RuO_2 is really formed during the XPS sampling procedure or in the preparation of NFS-Ru(0). For this purpose we analyzed NFS-Ru(0) by Raman spectroscopy, which is a strong tool to test the existence of RuO_2. It was observed that the characteristics Raman peaks of RuO_2 (see ref 27b and c) in the range 400−1200 cm^{-1} were missing in the Raman spectrum of NFS-Ru(0), which confirms that the detection of RuO_2 by XPS is a result of the surface oxidation of ruthenium(0) nanoclusters during the XPS sampling procedure.

(23) Wilkins, R. G. *Kinetics and Mechanism of Reactions of Transition Metal Complexes*, 2nd ed.; VCH: New York, 1991.
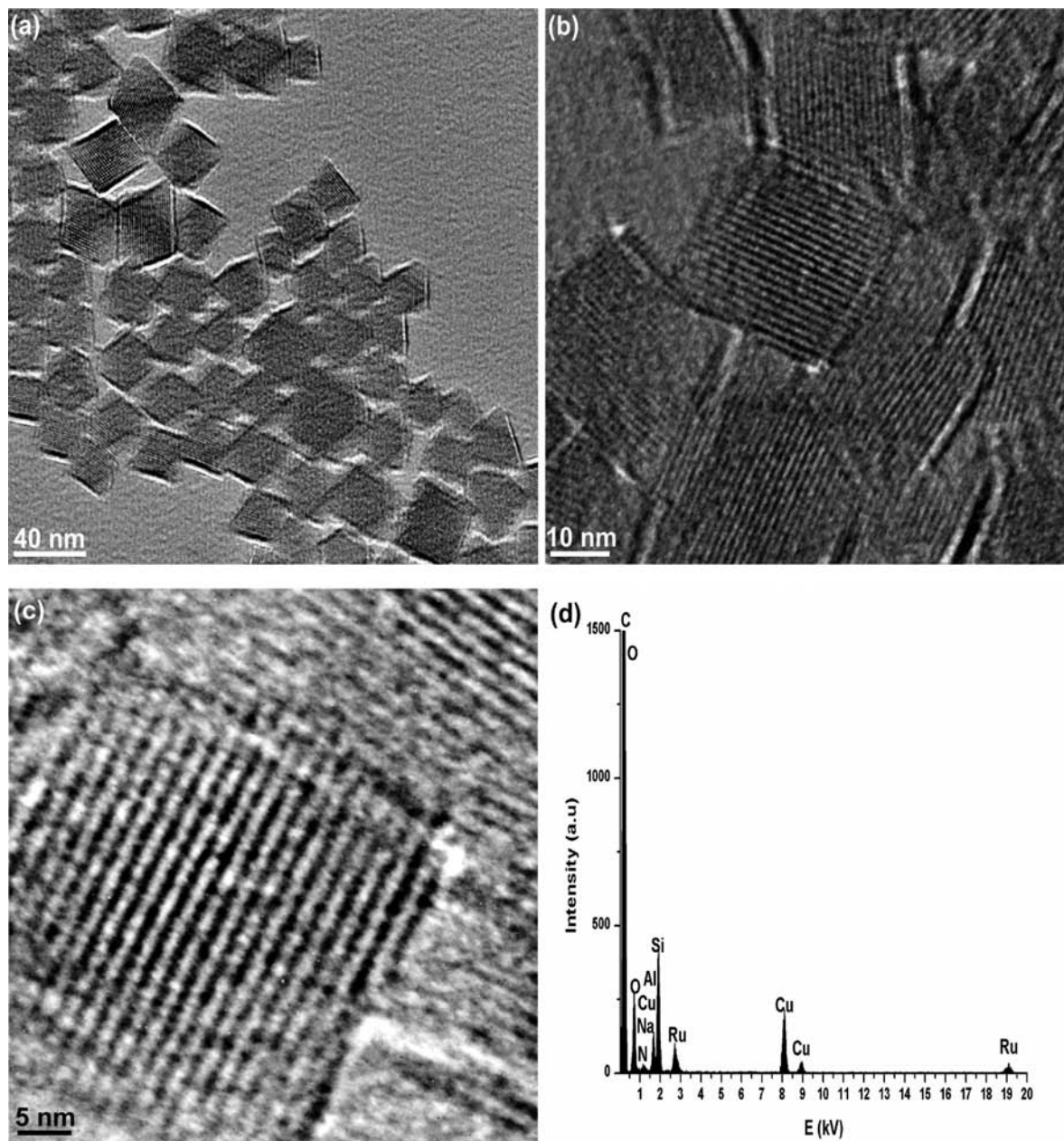
Figure 1. (a and b) TEM images of NFS-Ru(0) with different magnifications, (c) high resolution TEM image of NFS-Ru(0), and (d) TEM-EDX spectrum of NFS-Ru(0).

electronic properties of the zeolite matrix.[31] The interaction of ruthenium(0) nanoclusters with the framework oxygen of zeolite is expected to induce a positive charge on the surface metal which would increase the binding energies of ruthenium(0) nanoclusters. A similar effect has also been observed for the zeolite encapsulated cobalt[31a] and platinum.[31c] In addition to matrix effect, the high energy shifts in the ruthenium binding

energies might be due to the fact that electrons in the core level are strongly restricted by the atomic nucleus as observed in the case of palladium(0) nanoclusters in zeolite-Y.[32]

In the characterization of zeolite confined metal(0) nanoclusters, far-IR spectroscopy is a direct probe for location of cation sites in zeolite via their characteristic vibrational modes.[33] The combined use of frequencies and intensities of the far-IR absorption bands due to the site specific cation translatory modes allows us to secure metal cation vibrational assignments for sites I, II, III, and I' in zeolite-Y (Figure 2a).[34] The far-IR assignment

(29) (a) Kim, H.; Popov, N. B. *J. Power Sources* **2002**, *104*, 52. (b) Liu, H. L.; Yoon, S.; Cooper, S. L.; Cao, G.; Crow, J. E. *Phys. Rev. B* **1999**, *60*, 6980. (c) Lee, S. H.; Liu, P.; Cheong, H. M.; Tracy, C. E.; Deb, S. K. *Solid State Ionics* **2003**, *165*, 217.

(30) Schmid, G., Ed. *Clusters and Colloids; From Theory to Applications*; VCH Publishers: New York, 1994.

(31) (a) Guczi, L.; Bazin, D. *Appl. Catal., A* **1999**, *188*, 163. (b) Jiang, Y.-X.; Weng, W.-Z.; Si, D.; Sun, S.-G. *J. Phys. Chem. B* **2005**, *109*, 7637. (c) Fukuoko, A.; Higashimoto, N.; Sakamoto, Y.; Inagaki, S.; Fukushima, Y.; Ichikawa, M. *Top. Catal.* **2002**, *18*, 73.

(32) Okitsu, K.; Yue, A.; Tanabe, S.; Matsumoto, H. *Bull. Chem. Soc. Jpn.* **2002**, *75*, 449.

(33) Baker, M. D.; Godber, J.; Ozin, G. A. *J. Am. Chem. Soc.* **1985**, *107*, 3033.

(34) Özkar, S.; McMurray, L.; Holmes, A. J.; Kuperman, A.; Ozin, G. A. *J. Phys. Chem.* **1991**, *95*, 9448.
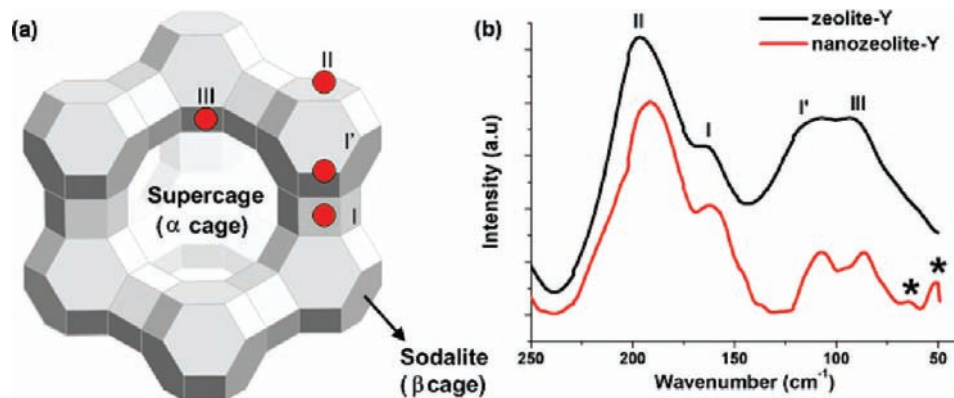
Figure 2. (a) Schematic view of the structure of the zeolite-Y (FAU framework); (b) Far-IR spectra of zeolite-Y (upper, black) and nanozeolite-Y powders (down, red) taken from the self-supporting wafers dehydrated in vacuum (10^{-7} Torr) at 550 °C. Asterisks denote the bands attributed to the tetramethylammonium cation (TMA$^+$) translatory modes in the spectrum of nanozeolite-Y.

of the extra-framework cation sites in zeolite-Y has also been confirmed by ^{23}Na NMR spectroscopy.[35] It has been shown that there are normal modes of the charge balancing cations, essentially decoupled from the lattice vibrations,[33] and each cation site has a vibrational mode with a characteristic frequency in the far-IR region. The frequencies of cation translatory vibrational modes depend on the mass and charge of the cation.[33] The far-IR spectra of nanozeolite-Y and zeolite-Y samples, both thermally dehydrated, are depicted together in Figure 2b for comparison. The far-IR spectrum of nanozeolite-Y shows two lower frequency bands at 65 and 52 cm^{-1} which are readily assigned to the translatory modes of the residual tetramethylammonium cation, TMA$^+$.[36] On passing from nanozeolite-Y to ruthenium(III)-exchanged nanozeolite-Y, the site II and III Na$^+$ cation bands in the far-IR spectra (Figure 3a) lose intensity while two lower frequency bands grow in at 69 and 55 cm^{-1}, which can be assigned to the Ru^{3+} cation translatory modes in sites II and III. The higher frequency absorption band at 69 cm^{-1} is most likely due to the site II Ru^{3+} cation mode, and the lower frequency absorption band at 55 cm^{-1} is attributed to the site III Ru^{3+}. This result indicates that site II and site III Na$^+$ cations in the supercage (α-cage) are replaced by ruthenium(III) cations. It is noteworthy that after ion exchange the absorption bands of the remaining Na$^+$ and TMA$^+$ ions are shifted to higher frequencies due to the change in binding strength affected by the specific site population.[19,33,34] In the far-IR spectrum of NFS-Ru(0) depicted in Figure 3b, one observes that the cation sites II and III left vacant by Ru^{3+} ions upon reduction are reoccupied by Na$^+$ cations coming from sodium borohydride. Obtaining the absorption bands for NFS-Ru(0) essentially at the same frequency and intensity as the ones in the spectrum of virgin nanozeolite-Y (Figure 3b) indicates that the host material retains its integrity including the cation site population after the generation of ruthenium(0) nanoclusters within the supercages of a nanozeolite.
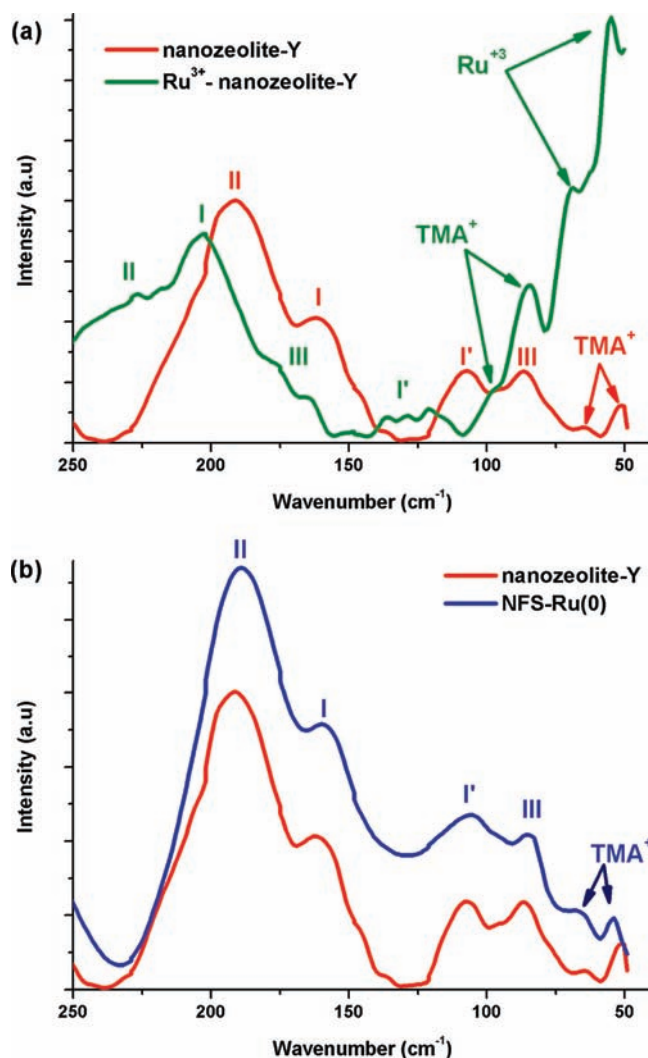
(35) (a) Jelinek, R.; Özkar, S.; Ozin, G. A. *J. Am. Chem. Soc.* **1992**, *114*, 4907. (b) Jelinek, R.; Özkar, S.; Ozin, G. A. *J. Phys. Chem.* **1992**, *96*, 5949. (c) Jelinek, R.; Özkar, S.; Pastore, H. O.; Malek, A.; Ozin, G. A. *J. Am. Chem. Soc.* **1993**, *1145*, 563. (d) Ozin, G. A.; Özkar, S.; Macdonald, P. *J. Phys. Chem.* **1990**, *94*, 6939.
(36) Note that all the nanozeolite samples used in this study were subjected to ion exchange without calcination and, therefore, may contain residual TMA$^+$ cations used as a template in the synthesis of nanozeolite. The heavier TMA$^+$ cations are expected to have lower frequency translatory vibrational modes than those of Na$^+$ cations. The residual TMA$^+$ cations, which are difficult to remove by thermal dehydration in vacuum, are most probably in sites I and I′ (in sodalite cages).

Figure 3. Far-IR spectra of (a) nanozeolite-Y (red) and ruthenium(III)-exchanged nanozeolite-Y (green) as well as (b) nanozeolite-Y (red) and NFS-Ru(0) (blue) formed from the sodium borohydride reduction of ruthenium(III)-exchanged nanozeolite-Y.

Catalytic Activity of Ruthenium(0) Nanoclusters Stabilized by a Nanozeolite Framework in the Hydrogenation of Neat Aromatics under Mild Conditions. The catalytic activity of NFS-Ru(0) was tested in the hydrogenation of aromatics (benzene,
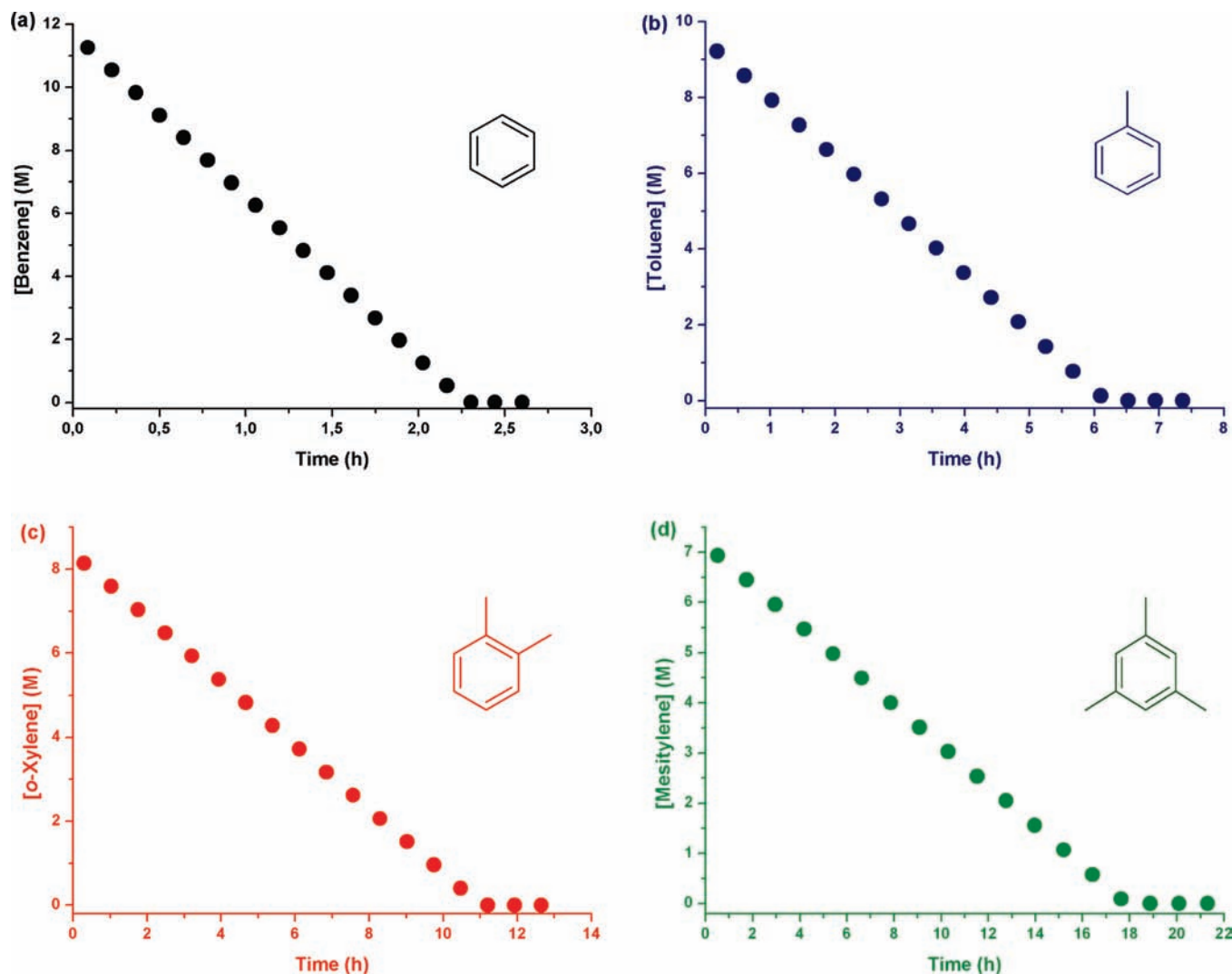
Figure 4. Graphs of concentration of (a) benzene, (b) toluene, (c) *o*-xylene, and (d) mesitylene versus time for hydrogenation of 1.0 mL of neat substrate catalyzed by 100 mg of NFS-Ru(0) (with a ruthenium loading of 0.27% wt corresponding to 2.7 μmol of Ru) at 25 $\pm$ 0.1 °C and 42 $\pm$ 1 psig initial H$_2$ pressure.

toluene, *o*-xylene, and mesitylene) in the solvent-free systems. An important observation is that when the mostly hydrophilic NFS-Ru(0) are dispersed in an organic medium they lose their colloidal stability while their framework preserves its crystallinity as confirmed by XRD (see Figure S-4 in the Supporting Information). Although the nanozeolites are gathering to form clumps in the organic medium, ruthenium(0) nanoclusters retain their stability and do not show any agglomeration into the bulk ruthenium as evidenced by TEM analyses (see Figure S-5 in the Supporting Information). The catalytic hydrogenation of aromatics in the solvent-free system was started by agitating the NFS-Ru(0) in the aromatic substrate at 25 $\pm$ 0.1 °C and 42 $\pm$ 1 psig H$_2$, and the progress of the reaction was followed by monitoring the hydrogen uptake which can be converted to the concentration loss of the aromatic substrate by using the stoichiometry. The complete hydrogenation of aromatics was also confirmed by checking the ^{1}H NMR spectra of the reaction solution at the end of the reaction. Figure 4 shows the plots of concentration loss of aromatics vs time for the hydrogenation of neat aromatics (benzene, toluene, *o*-xylene, and mesitylene) catalyzed by NFS-Ru(0). For all of the substrates the hydrogenation starts immediately without an induction period as a preformed catalyst is used. A linear hydrogenation continues

until the consumption of benzene, toluene, *o*-xylene, and mesitylene with *initial* TOF values[37] of 5430, 1800, 870, or 460 h^{-1}, respectively. The TOF of 5430 h^{-1} for the complete hydrogenation of neat benzene, a well-known test reaction in arene hydrogenation, is the record value since the highest TOF previously reported for the hydrogenation of neat benzene under mild conditions ($\leq$25 °C and $\leq$3 atm) is 1040 h^{-1} (see Table S-1 in the Supporting Information).[12] It is also noteworthy that NFS-Ru(0) provide a significant improvement in catalytic activity in the hydrogenation of neat benzene compared to the results reported for ruthenium(0) nanoclusters supported on nonporous silica[38] or mesoporous silica.[39]

---

(37) The TOF and TTO values reported herein are those typically reported. TOF = (mol of H$_2$ consumed/total mol of catalyst loading)/time; TTO = (TOF) (time). That is, the reported values of TOF and TTO are not corrected for the amount of metal that is on the surface of the catalyst and/or the actual number of active sites. For the calculation of initial TOF values the conversions of substrates within the first hour were considered.

(38) Ruthenium(0) nanoclusters supported on silica provide a TOF value of 864 h^{-1} in the hydrogenation of benzene to cyclohexane under forcing conditions (at 140 °C and 870 psig H$_2$ pressure). Ning, J.; Xu, J.; Liu, J.; Lu, F. *Catal. Lett.* **2006**, *109*, 175.
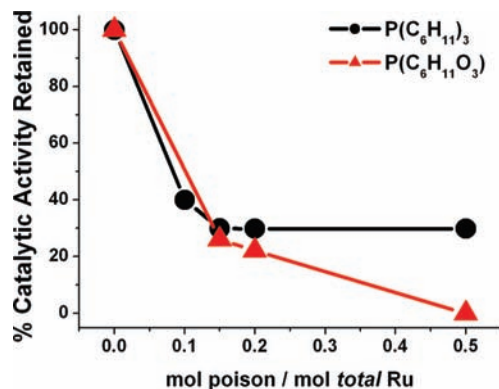
Figure 5. Plots of the relative catalytic activity of NFS-Ru(0) retained versus mol poison/*total* mol Ru ratio for the $P(C_6H_{11})_3$ and $P(C_6H_{11}O_3)$ poisoning in the hydrogenation of 1.0 mL of neat benzene catalyzed by 100 mg of NFS-Ru(0) (with a ruthenium loading of 0.27% wt corresponding to 2.7 μmol Ru) at 25 ± 0.1 °C and 42 ± 1 psig initial H_2 pressure.

In the series of benzene, toluene, *o*-xylene, and mesitylene, the hydrogenation rate decreases with the increasing number of methyl substituents, because of the electronic effect on the aromatic ring due to the addition of methyl groups.[40] Additionally, the observation of the slowest hydrogenation rate for mesitylene can also be explained by the Lennard−Jones kinetic diameter of mesitylene (7.6 Å),[22] which is larger than the supercage aperture of nanozeolite-Y (7.4 Å).[22]

$P(C_6H_{11})_3$ and $PC_6H_{11}O_3$ Poisoning of Nanozeolite Framework Stabilized Ruthenium(0) Nanoclusters in the Hydrogenation of Neat Benzene. In working with the zeolite confined metal particles, the crucial question is whether the nanoclusters are on the surface or in the cavities of the host material. To investigate the distribution of ruthenium(0) nanoclusters on the external surface or within the cages of nanozeolite-Y, a series of poisoning experiments for the hydrogenation of neat benzene catalyzed by NFS-Ru(0) were performed by using two different phosphine ligands as poison: tricyclohexylphosphine, $P(C_6H_{11})_3$, and 4-ethyl-2,6,7-trioxa-1-phosphabicyclo[2.2.2]octane, $P(C_6H_{11}O_3)$, having kinetic diameters of 10.9 Å and 4.6 Å, respectively.[41] The hydrogenation of neat benzene catalyzed by NFS-Ru(0) was conducted in the presence of phosphine ligand in various phosphine/ruthenium molar ratios at 25.0 ± 0.1 °C. The initial rate of benzene hydrogenation was determined in each of the independent experiments at various phosphine/ruthenium ratios and divided by the hydrogenation rate of neat benzene in the absence of phosphine at 25.0 ± 0.1 °C to obtain the catalytic activity retained (initial rate of benzene hydrogenation in the presence of poison over the one in the absence of poison). Figure 5 shows the plots of the percent catalytic activity retained in the hydrogenation of neat benzene versus the phosphine/ruthenium molar ratio for both of the phosphine poisons. In the hydrogenation experiments performed in the presence of $P(C_6H_{11}O_3)$, the catalytic activity of NFS-Ru(0) decreases almost

linearly with the increasing concentration of phosphine and the hydrogenation stops when 0.50 equiv of $P(C_6H_{11}O_3)$ per ruthenium is added to benzene (Figure 5). The observation that the benzene hydrogenation is completely poisoned by less than 1 equiv of phosphine is compelling evidence for a heterogeneous catalysis.[42] In the experiments with $P(C_6H_{11})_3$ the activity of the catalyst in the hydrogenation of neat benzene also decreases initially with the increasing phosphine/ruthenium molar ratio up to 0.15 and then remains unchanged beyond this ratio. The dissimilarity of two phosphine ligands in poisoning the NFS-Ru(0) catalyst in the hydrogenation of neat benzene arises from their size difference. While the small phosphine $P(C_6H_{11}O_3)$ (kinetic diameter is 4.6 Å) can readily enter the supercages through the 7.4 Å aperture of nanozeolite,[22] the large phoshine $P(C_6H_{11})_3$ (kinetic diameter is 10.9 Å) cannot enter the nanozeolite cages, thus remaining outside. Therefore, the large $P(C_6H_{11})_3$ can poison only the ruthenium(0) nanoclusters on the external surface of the nanozeolite, while the small $P(C_6H_{11}O_3)$ deactivates all the ruthenium(0) nanoclusters in the cavities and on the external surface of the zeolite. The results of these experiments given in Figure 5 indicate that the NFS-Ru(0) sample has 70% of the catalytically active ruthenium(0) nanoclusters standing on the external surface of the nanozeolite while the remaining 30% are in the cavities of the nanozeolite.

Catalytic Lifetime of Nanozeolite Framework Stabilized Ruthenium(0) Nanoclusters in the Hydrogenation of Neat Benzene under Mild Conditions. The catalytic lifetime of NFS-Ru(0) in the hydrogenation of neat benzene was determined by measuring the total turnover number (TTO) at 25 ± 0.1 °C and 42 ± 1 psig initial H_2 pressure. When all of the benzene was converted to cyclohexane, more benzene was added into the solution and the reaction was continued in this way until no hydrogen uptake was observed. It was found that NFS-Ru(0) provide 177 200 turnovers in benzene hydrogenation over 105 h before deactivation (see Figure S-6 in the Supporting Information). The *average* TOF value during this lifetime experiment is 1690 h^{-1} which is approximately one-third of the *initial* TOF value of 5430 h^{-1} indicating that the nanoclusters are deactivated as the catalytic reaction proceeds. The decrease in the catalytic activity of ruthenium(0) nanoclusters over time may be attributed to the gathering of nanozeolite particles to form clumps in the organic medium as evidenced by TEM analyses (*vide supra*) which decreases the accessibility of ruthenium(0) nanoclusters confined within the cages of nanozeolites.

Nevertheless, this is the highest TTO value ever reported in the hydrogenation of neat benzene, 70 times larger than the previous best value.[12]

Isolability and Reusability of Nanozeolite Framework Stabilized Ruthenium(0) Nanoclusters in the Hydrogenation of Neat Benzene under Mild Conditions. Isolability and reusability of NFS-Ru(0) were also tested in the hydrogenation of neat benzene. After the complete hydrogenation of neat benzene, the catalyst was isolated as black powders and bottled under a nitrogen atmosphere. The isolated NFS-Ru(0) are redispersed in benzene and yet an active catalyst in benzene hydrogenation. They retain 92% of their initial activity for the third run in the hydrogenation of neat benzene with complete conversion into cyclohexane (see Figure S-7 in the Supporting Information). This indicates that NFS-Ru(0) are an isolable, bottleable, redispersible, and reusable catalyst in the hydrogenation of

(39) Ruthenium(0) nanoclusters supported on mesoporous silica provide a TOF value of 3600 h^{-1} in the hydrogenation of benzene to cyclohexane under forcing conditions (at 110 °C and 580 psig H_2 pressure). Su, F.; Lv, L.; Yin, F.; Tao-Liu, T.; Cooper, A. I.; Song-Zhao, A. *J. Am. Chem. Soc.* **2007**, *129*, 14213.

(40) (a) March, J. *Advanced Organic Chemistry: Reactions, Mechanisms, and Structure*, 4th ed.; Wiley-Interscience: New York, 1992. (b) Fonseca, G. S.; Silveira, E. T.; Gelesky, M. A.; Dupont, J. *Adv. Synth. Catal.* **2005**, *347*, 847. (c) Bahaman, M. V.; Vannice, M. A. *J. Catal.* **1991**, *127*, 251.

(41) Li, X.; Ozin, G. A.; Ozkar, S. *J. Phys. Chem.* **1991**, *95*, 4463.

(42) (a) Lin, Y.; Finke, R. G. *Inorg. Chem.* **1994**, *33*, 4891. (b) Hornstein, B. J.; Aiken, J. D., III.; Finke, R. G. *Inorg. Chem.* **2002**, *41*, 1625.

aromatics in a solvent-free system under mild conditions. Additionally, no ruthenium was detected (by ICP, detection limit 24 ppb for Ru) in the filtrate obtained by filtration of the reaction mixture after the first run of hydrogenation. The results of this leaching test confirms the retaining of ruthenium within the zeolite matrix (no ruthenium passes into the solution during the suction filtration). A control experiment was also performed to show that the hydrogenation of benzene is completely stopped by the removal of NFS-Ru(0) from the reaction solution.

Conclusions

The main findings of this work as well as implications or predictions can be summarized as follows:

(1) The colloidal nanozeolite framework stabilized ruthenium(0) nanoclusters were prepared for the first time as a new material and characterized by using ICP-OES, XRD, DLS, TEM, HRTEM, TEM-EDX, XPS, mid-IR, far-IR, and Raman spectroscopy. The results of these multiprong analyses reveal the formation of ruthenium(0) nanoclusters within the framework of well-dispersed colloidal nanozeolite particles whereby the host material retains its integrity including the cation site population after the generation of ruthenium(0) nanoclusters within the supercages of the nanozeolites.

(2) The dispersion of nanozeolite framework stabilized ruthenium(0) nanoclusters in the aromatic substrates acts as a superb catalyst in terms of activity, selectivity, and lifetime in the solvent-free hydrogenation of aromatics under mild conditions. They provide a record TTO of 177 200 and TOF up to 5420 h^{-1} in the hydrogenation of neat benzene with 100% conversion and selectivity to cyclohexane at 25 ± 0.1 °C and with an initial H$_2$ pressure of 42 ± 1 psig. Recall that the prior highest TTO and TOF values are 2420 mol H$_2$·(mol Ru)$^{-1}$ and 1040 h^{-1}, respectively.[12] Moreover, they show also exceptional catalytic activity in the solvent-free hydrogenation of toluene, *o*-xylene, and mesitylene with 100% conversion and TOF values of 1800, 870, and 580 h^{-1}, respectively.

(3) The complete hydrogenation of neat benzene is achieved even in successive runs performed by redispersing the NFS-Ru(0) isolated after the previous run. When reused, NFS-Ru(0) retain 92% of their initial catalytic activity even for the third run with a complete hydrogenation of benzene to cyclohexane. Thus, they are an isolable, bottleable, and reusable catalyst in the hydrogenation of neat benzene at 25 ± 0.1 °C with an initial H$_2$ pressure of 42 ± 1 psig.

(4) The poisoning experiments using small and large phosphines were performed to address the crucial issue of whether the nanoclusters are on the surface or in the cavities of the host material. The results of these experiments reveal that 70% of active ruthenium(0) nanoclusters are on the external surface of nanozeolite particles while only 30% of ruthenium(0) nanoclusters are in the supercages of the zeolite.

(5) The solvent-free hydrogenation of aromatics catalyzed by NFS-Ru(0) is "relatively green" in terms of its environmental impact as it fulfills 7 of the 12 requirements of green chemistry[20] including the following: (*i*) it is 100% selective and minimizes byproducts or waste; (*ii*) it maximizes the incorporation of all reactants into the products; (*iii*) it is solventless (i.e., uses neat aromatics as the substrate/solvent); (*iv*) it requires relatively low energy as it occurs under mild conditions of 25.0 ± 0.1 °C and ≤3 atm of pressure; (*v*) it is catalytic, not stoichiometric; (*vi*) it does not use any blocking, protecting/deprotecting group; (*vii*) real-time monitoring is easy by measuring the H$_2$ uptake, ^{1}H NMR, or GC analysis, for example.

Supporting Information Available: Table S-1: The top 17 catalysts in benzene hydrogenation at room temperature. Figure S1: X-ray diffraction patterns of nanozeolite and nanozeolite framework stabilized ruthenium(0) nanoclusters with a ruthenium content of 0.27% wt. Figure S2: Particle size distribution and its fit obtained from the dynamic light scattering analysis of the nanozeolite framework stabilized ruthenium(0) nanoclusters with a ruthenium content of 0.27% wt. Figure S3: (a) XPS survey scan spectrum, (b) high resolution Ru 3d XPS spectrum and its simulated peak fitting in the region 279−292 eV, (c) high resolution Ru 3p XPS spectrum and its simulated peak fitting in the region 470−450 eV of the nanozeolite framework stabilized ruthenium(0) nanoclusters with a Ru content of 0.27% wt. Figure S4: X-ray diffraction pattern of nanozeolite framework stabilized ruthenium(0) nanoclusters recovered after the hydrogenation of 1.0 mL of benzene starting with 100 mg of NFS-Ru(0). Figure S5: TEM images of the nanozeolite framework stabilized ruthenium(0) nanoclusters with a Ru content of 0.27% wt dispersed in neat benzene at room temperature. Figure S6: Graph of benzene consumption versus time for the hydrogenation of neat benzene catalyzed by the nanozeolite framework stabilized ruthenium(0) nanoclusters. Figure S7: The percentage of catalytic activity and conversion versus the number of catalytic runs for the hydrogenation of 1.0 mL of benzene (11.2 mmol), catalyzed by NFS-Ru(0) (0.27% wt Ru, 100 mg, 2.7 μmol of Ru) at 25 ± 0.1 °C with an initial H$_2$ pressure of 42 ± 1 psig. This material is available free of charge via the Internet at http://pubs.acs.org.

JA101602D